Carbohydrate Polymers 98 (2013) 372–379

Contents lists available at SciVerse ScienceDirect

Carbohydrate Polymers

journal homepage: www.elsevier.com/locate/carbpol

Scanning probe acoustic microscopy of extruded starch materials: Direct visual evidence of starch crystal

Zhongdong Liu [a,*], Boxiang Liu [b], Mengxing Li [a], Min Wei [a], Hua Li [a], Peng Liu [c], Tuo Wan [a]

[a] College of Food Science and Technology, Henan University of Technology, South Songshan Road 140#, Zhengzhou 450052, PR China
[b] Illinois Wesleyan University, Bloomington, IL, USA
[c] Faculty of Chemical Engineering and Light Industry, Guangdong University of Technology, Guangzhou 510090, PR China

ARTICLE INFO

Article history:
Received 24 April 2013
Received in revised form 14 May 2013
Accepted 15 May 2013
Available online 22 May 2013

Keywords:
Starch
SPAM
Microcrystal
Visual evidence

ABSTRACT

Scanning probe acoustic microscopy (SPAM) has been successfully used to study inorganic and keratin biomaterials. However, few studies have attempted to apply SPAM to structural study of non-keratin organic materials such as starch based materials. This study investigated hardness and surface finish to establish sample preparation method suitable for SPAM imaging and acquired clear acoustic images of extruded starch materials. Acquired acoustic images directly exhibited certain structure of starch materials and provided visual evidence of starch material components and aggregates. In addition, through correlating acoustic images with X-ray diffraction data, crystal-structural information in nano-scale was obtained and acoustic image contrast showed a linear relationship with starch amylose content in extruded starch materials.

© 2013 Elsevier Ltd. All rights reserved.

1. Introduction

Sonic wave has contributed significantly to the advancement of imaging technology. The wavelength and energy of a sonic wave determine its interaction with matter. For instance, we could hear through vibration of hair cells caused by sonic wave. Similarly, when sonic waves are absorbed by, pass through or reflect off of an object, data could be recorded by receptors in different degree and translated into images. We can then "see" the object and obtain information of the surface and internal structure of the objective. However, in order to probe the object or resolve two objects, the wavelength of sonic waves should be equivalent to or shorter than the size of an object or the distance between two objects. Recent progress in scanning probe acoustic microscopy (SPAM) has made it possible for sonic wave to be employed to probe nano-scale structure and to be used alongside atomic force microscopy (AFM).

Starch is a natural, renewable, and biodegradable polymer produced by many plants as a source of stored energy (Le Corre, Bras, & Dufresne, 2010). Apart from being used as a staple food component for human metabolism, it is also widely developed to be industrial materials. For instance, various kinds of alcohol have been extracted from starch to be green fuel. And starch structure has been under research for many years. The morphology of natural starch-micro-scale globular and polygonal particles of starch had been confirmed with electron microscopy. Under a polarized light microscope, cereal starches exhibited internal anisotropic structure (Hug-Iten, Handschin, Conde-Petit, & Escher, 1999). X-ray analysis revealed the degree of crystallinity of starch to be between 15% and 45% (Zobel, 1988). Starch based materials of different properties (such as different crystal structure and elastoplasticity) could be fabricated through the components modulation and processing. For the study of starch structure, microscopy technology illustrated the structure of starch material with images, polarized microscopy helped us observe the polarized cross of natural starch granules, helped us observe the morphology of natural starch and starch material was characterized with electron microscopy technology including transmission electron microscopy (TEM) and scanning electron microscopy (SEM) (Gallant, Bouchet, & Baldwin, 1997). Scanning probe microscopy had advanced the study of structure into nano-scale and the intermediate structure of natural starch granules were directly observed (An, Liang, & Liu, 2011; Thiré, Simão, & Andrade 2003) Atomic force microscopy (AFM) helped confirm the nanounit chains and "blocklets" of natural starch granules, which were only hypotheses before (Baldwin, Adler, Davies, & Melia, 1998; Guo, Liu, An, Li, & Hu, 2011; Li, Liu, & Liu, 2009; Ridout, Gunning, Parker, Wilson, & Morris, 2002).

However, till now there is no microscopy technology capable of confirming the crystal structure of starch materials. X-ray diffraction has always been regarded as a useful tool to study crystal structure of starch. Nevertheless, X-ray diffraction data of starch material are hard to explain exactly or correlate with accurate

* Corresponding author. Tel.: +86 13837160861; fax: +86 37167788125.
E-mail address: liuzhongdong@haut.edu.cn (Z. Liu).

0144-8617/$ – see front matter © 2013 Elsevier Ltd. All rights reserved.
http://dx.doi.org/10.1016/j.carbpol.2013.05.029

crystalline aggregates and crystal morphology of starch materials. This may result from the less organized spatial arrangement of microcrystal and incomplete microcrystal organization. The most important problem is that starch crystal structure could not be directly observed from X-ray diffraction patterns. For instance, X-ray diffraction patterns could not tell us how different crystal components distribute or combine when starch formed solid materials. Starch crystal structure information calculated from X-ray diffraction data could not be verified by visual images, thus there is still a lack of clear understanding of starch surface and internal structure.

Acoustic microscopy has progressed greatly in recent years. It has been successfully applied in material science, especially in the analysis of various opaque materials. Not only could acoustic microscopy be used to observe the surface, subsurface and internal microstructure of materials, but it could characterize the physical properties of materials aided by $V(Z)$ curves. To our knowledge, this study is the first to establish the preparation method suitable for acquiring clear acoustic images of extruded starch samples. Using SPAM, the crystal aggregates of starch structure were characterized directly for the first time. SPAM helped us to image three different starch samples (CS, G50, WAXY), each containing different amylose and amylopectin content. After correlating X-ray diffraction data of extruded starch materials with acoustic images, the crystalline structural information in the images was explained and the relationship between image contrast and starch components was analyzed.

2. Materials and methods

2.1. Materials

Extruded starch samples WAXY (amylose content = 0%), MAIZE (amylose content = 26%) and G50 (amylose content = 50%) were provided by South China University of Technology, PR China.

2.2. SPAM imaging

2.2.1. Samples preparation

We have tried different methods for two years to acquire clear images of starch by SPAM imaging. Preforming and film preparation methods were used to process starch and we failed to obtain clear acoustic images. During these trials, we found that high quality SPAM images could be obtained only if starch samples met the requirements in hardness and surface finish. Therefore we employed extrusion technique to process samples to make hardness and surface finish suitable for SPAM imaging.

2.2.2. Polishing extruded starch samples

Upper and bottom surfaces of cylindrical extruded starch samples WAXY, MAIZE and G50 were polished with heavy-grade sandpaper, finer-grade sandpaper, silk and glass slide to make upper and bottom surface smooth and parallel. Different samples were processed to the same roughness of 3–9 μm.

2.2.3. Measuring hardness

Vickers hardness measurement were conducted by indenting cross sections of the extruded starch samples at a load of 0.98 N using a MHV2000 digital Vickers hardness tester according to Eqs. (1) and (2).

$$\mathrm{HV} = \frac{0.189P}{d^2} \quad (1)$$

$$d = \frac{d_1 + d_2}{2} \quad (2)$$

Table 1
Bright region area in microscopy images of extruded starch samples (μm^2).

Polishing way	WAXY	CS	G50	Corn
Heavy-sand paper	439.2	302.2	901.1	389.8
Finer-sand paper	205.4	203.2	365.7	133.6
Silk	35.5	42.2	85.9	36.9
Glass slide	6.5	5.7	9.8	7.0

where P is the load (N) and the value is 9.807, d is the average of two indentation depth (d_1, d_2) of cross sections (mm).

2.2.4. Measuring surface finish

Extruded starch samples polished in different ways were taken photos with a ZEISS Imager. Alm upright metallographic microscope has amplification factors 100×, 200×, 500×, and 1000×, respectively. Clear images enlarged with the same amplification factor were processed statistically to observe the surface finish and starch granules. Bright region and granule projection region were circled in the images and measured using AXTO IMAGE software. Surface finish of extruded starch samples was represented by the accumulative bright region area and granule projection region area in one certain scale surface.

2.2.5. SPAM imaging condition

Samples polished in four ways were imaged using SPAM (Seiko Inc., Japan). After samples were glued on the transducer, AFM images were obtained through linear scanning. Acoustic imaging was obtained with frequency from 5 KHz to 100 KHz and with resolution 10 nm.

2.3. X-ray diffractometry of extruded starch samples

2.3.1. Samples preparation

Extruded starch samples were pulverized with a normal grinder and powders passed through a 56 mesh sieve. The pass-through was collected and ground with a mortar.

2.3.2. X-ray diffraction

X-ray diffraction was carried out on a BrukerD8-Focus X-ray diffractometer (Bruker AXS Corporation, Karlsruhe, Germany). Samples were ground and put on a glass slide (exclusive for X-ray diffractometry). Operating conditions were as follows:

X-ray source was a copper tube operating at 40 kV and 35 mA, producing CuKα radiation (λ = 1.5406 nm) and detector was Lynx-Eye semiconductor array transducer. Diffractograms were obtained by scanning from 4° (2θ) to 60° (2θ), diffracting from of 3° to 30°, a divergence slit width (DS) of 0.6°, a soller silt of 4°, and a scatter slit width (SS) of 3 mm.

3. Results and discussion

3.1. Correlations between SPAM imaging and surface finish of extruded starch samples

3.1.1. Acquired preparing conditions of extruded starch samples surface finish

Surface finishes of starch sample polished in four different ways were taken photos and 256 images were obtained. Four representative images amplified (500×) were picked out and showed in Fig. 1, and the surface finish was shown in Tables 1 and 2.

As clearly seen in the images in Fig. 1, the surface of starch samples polished with heavy-grade sandpaper (A), finer-grade sandpaper (B), silk (C) and glass slide (D) gradually changed from alternately shaded (A and B) to uniformly colored (C), and become smooth to mirror level (D). More than 7 regions within r = 1.5 mm

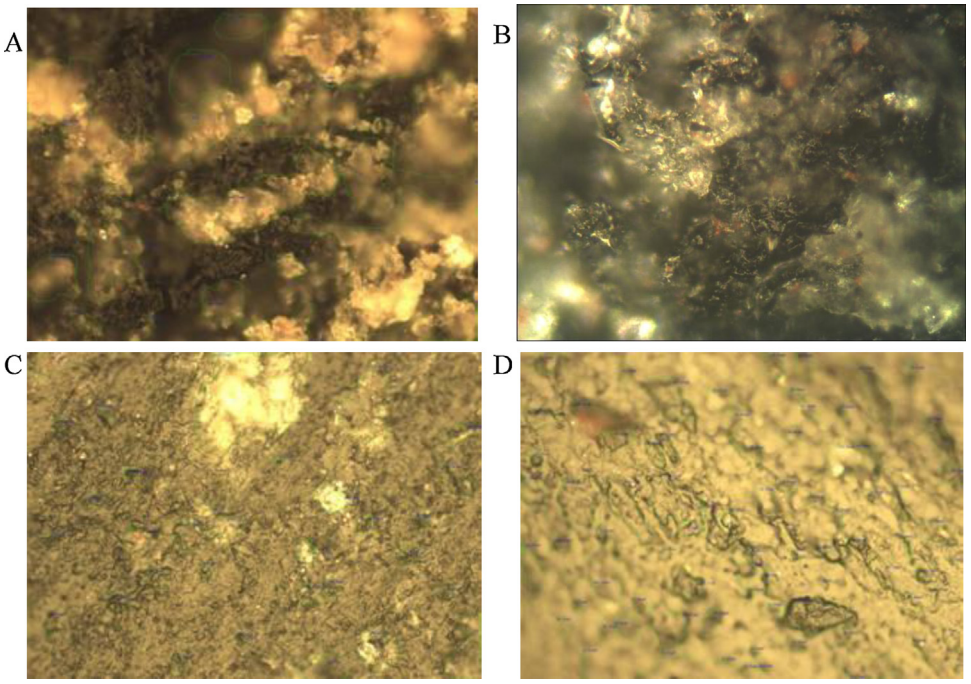

Fig. 1. Four images of extruded starch samples showed different surface finish. Images with amplification 500× of starch sample G50 polished with heavy-sandpaper (A), polished with finer-sandpaper (B), polished with silk (C) and polished with glass slide (D).

circle on the surface of samples were randomly picked out for statistical analysis, and data of acquired area of bright regions and particle projection regions were linked with the quality of SPAM images. We found that in the images of extruded starch samples with amplification 500×, if the area of bright region was 9.8 μm^2 larger than that of the G50 sample polished with silk, clear images could not be obtained.

As seen in the images, there appeared to be incomplete starch particles adhered to the surface of samples polished with heavy-sandpaper, finer-sandpaper and silk, while there were few particles adhered to the surface of starch samples polished with glass slide. This means that polishing not only made extruded starch smooth to mirror level, but helped the image surface much more clear and thus improved the images' quality. The interference stripes in the images (shown in Fig. 2) may emerge for the reason that starch particles fluctuate with the samples, splash and collide with the probe. The images became clear with a cleaner surface (shown in Fig. 3).

Statistical analysis of the direct surface images of extruded starch materials showed that to make the surface finish suitable for SPAM imaging of extruded starch samples smooth to mirror level, the area of accumulative bright regions within a $r = 1.5$ mm circle should be no more than 9.8 μm^2, and the accumulative particle projection area of the regions within a $r = 1.5$ mm circle should be no more than 0.3 μm^2.

3.1.2. Analysis of hardness of extruded starch samples

Hardness represents the capacity of resisting plastic deformation of material surface. As showed in Table 3, clear SPAM acoustic images of extruded starch samples could be obtained only if samples met the requirement of finish and the Vickers hardness value was over 166.

Table 2
Particle projection region area in microscopy images of extruded starch sample G50.

Sample G50	Area of particles projection region (μm^2)
Polished with heavy-sandpaper	57.3
Polished with finer-sandpaper	24.2
Polished with silk	4.4
Polished with glass slide	0.3

3.2. Correlations between acoustic image quality and surface finish of extruded starch samples

Confined to the length of this paper, representative images of sample corn were picked out and shown in Figs. 2 and 3. Clear images of extruded starch samples polished with heavy-sandpaper and finer-sandpaper could not be obtained. Images of extruded starch samples polished with silk and glass slide were illustrated in Figs. 2 and 3 separately.

The image quality was mainly determined by interference factors and image definition, acoustic image in Fig. 2 had interference stripes, resulting from interference factors while acoustic images in Fig. 3 was clear with few interference stripes.

Table 3
Vickers hardness of extruded starch samples.

Sample	d_1 (mm)	d_2 (mm)	HV	HV average
WAXY	95.156	96.227	202	201
	95.866	97.105	199	
	94.868	96.533	202	
Corn	99.313	103.813	180	175
	102.375	104.813	173	
	102.125	105.438	172	
G50	107.813	106.750	161	166
	105.688	106.500	165	
	102.500	105.188	172	
CS	98.675	99.883	189	188
	99.102	99.684	188	
	99.116	100.018	187	

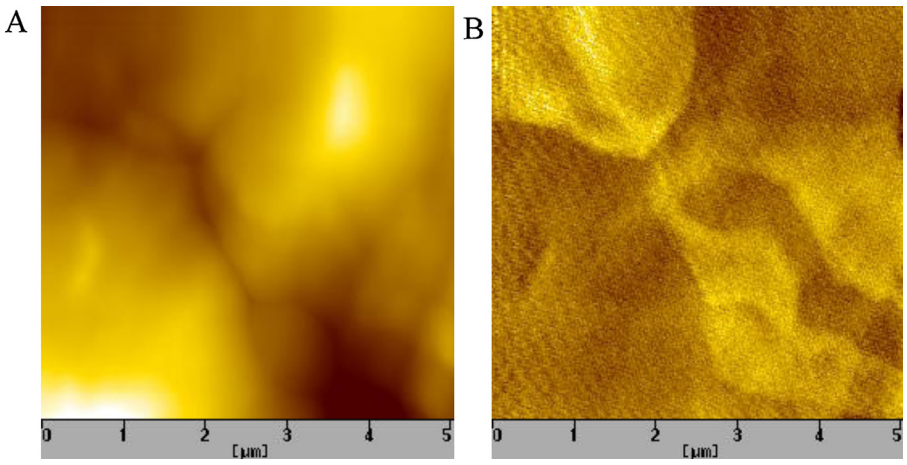

Fig. 2. Images of extruded starch sample corn polished with silk, surface topography image (A) and acoustic image (B).

3.3. SPAM images of extruded starch samples

SPAM imaging condition was established after investigating surface finish and hardness of extruded starch samples and SPAM images of samples containing different amylose content were shown in Fig. 4. From Figs. 3 and 4, left-hand images were AFM images overlaid with SPAM images of extruded starch samples. Concerning image quality, the definition and resolution of SPAM

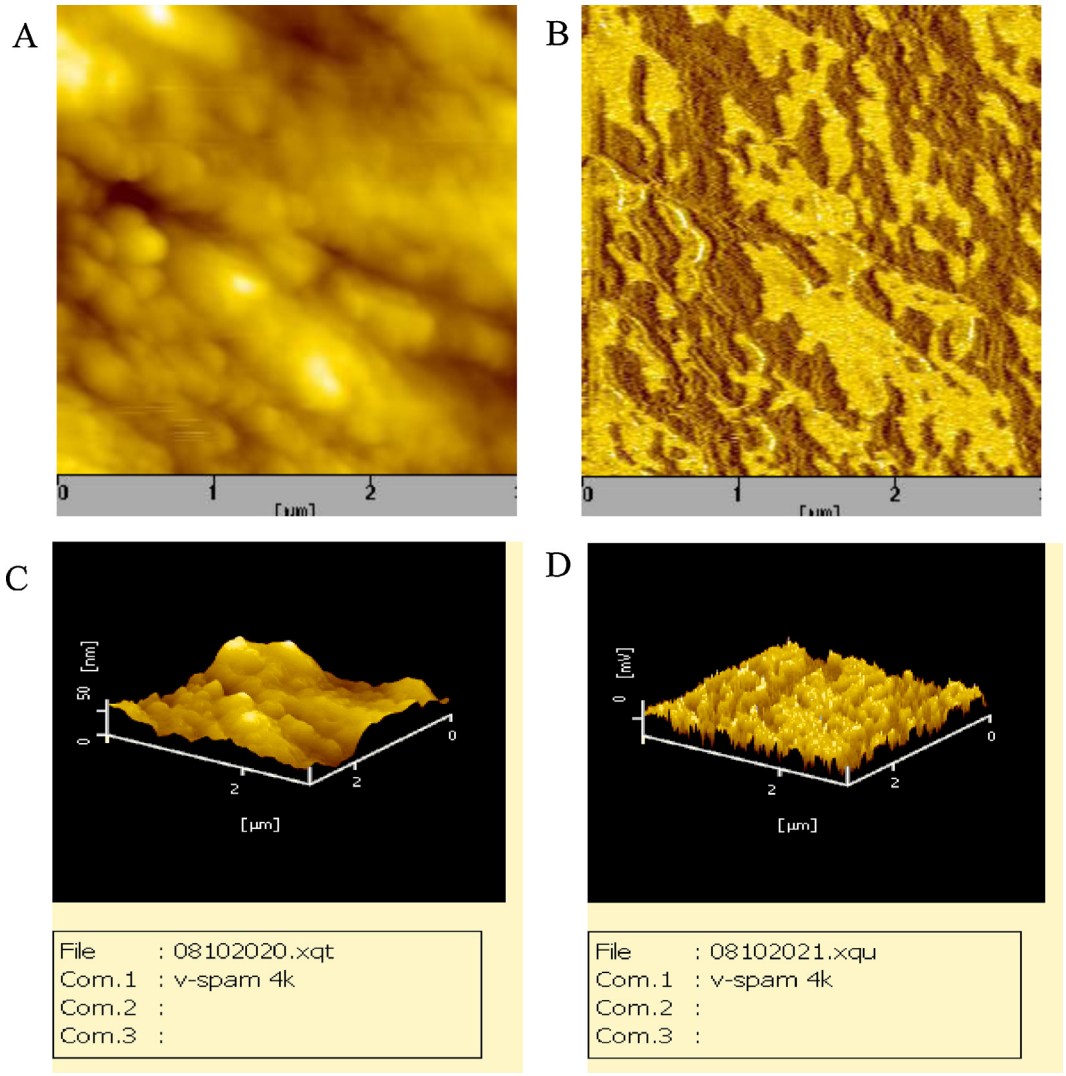

Fig. 3. Images of extruded starch sample corn polished with glass slide, surface topography image (A), acoustic image (B), three-dimensional surface topography image (C), and three-dimensional acoustic image (D).

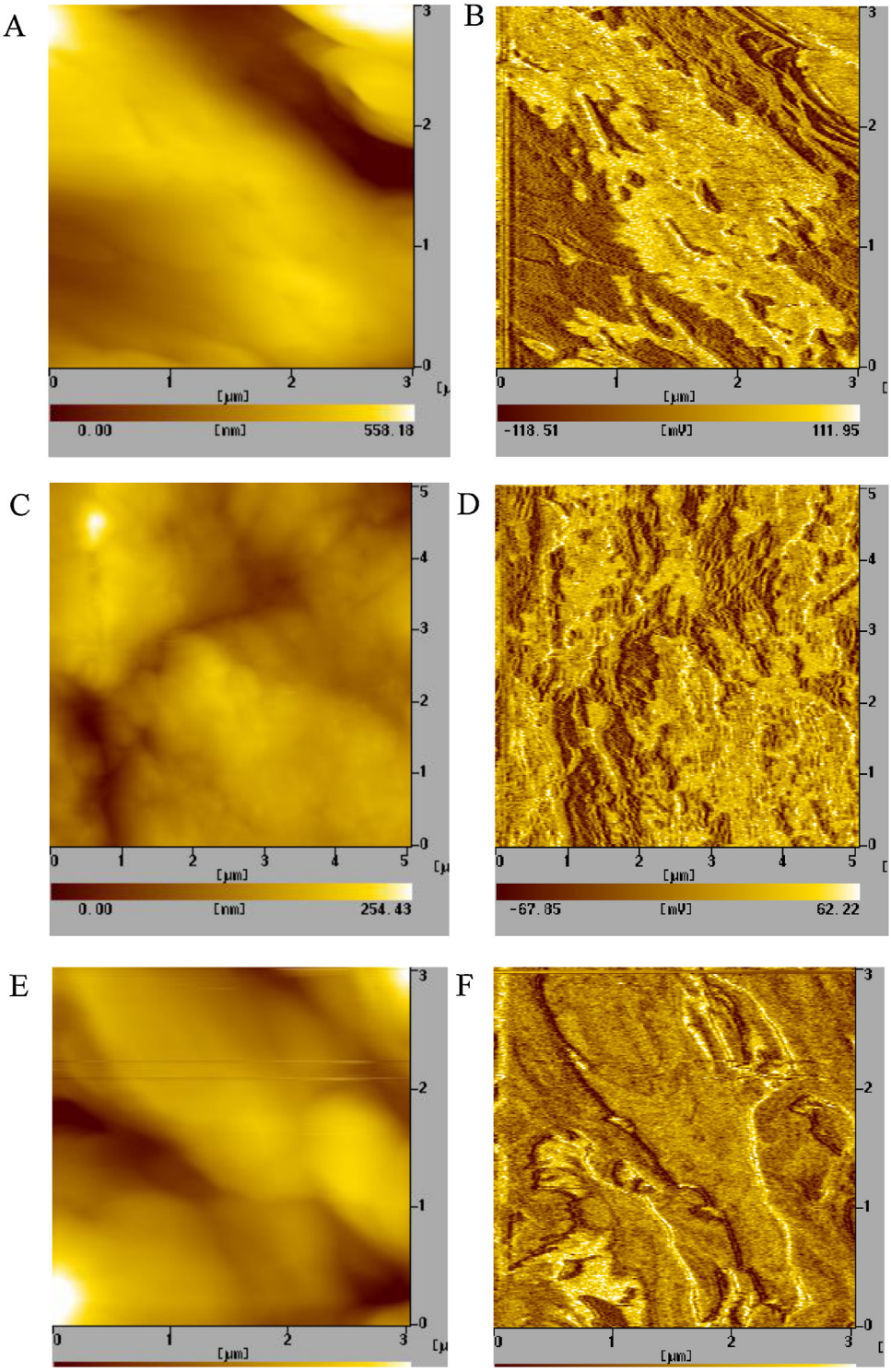

Fig. 4. SPAM images of extruded starch sample G50, surface topography image (A) and acoustic image (B); SPAM images of extruded starch sample CS, surface topography image (C) and acoustic image (D); SPAM images of extruded starch sample WAXY, surface topography image (E) and acoustic image (F).

images were better than AFM images. Besides, SPAM images contained information that AFM did not have: the same regions of starch samples showed different patterns in SPAM image and AFM image. According to imaging mechanism of SPAM, these patterns should be different crystals and aggregating states of starch materials. Starch crystals had always been deduced from indirect evidences before, but using SPAM had helped us obtain the direct image evidences of crystals in starch materials. It showed that starch crystals stood upright on the surface of starch material and aggregated in clusters in the three-dimensional SPAM images. Crystals distributed in various regions in the images and made up the "skeleton" of starch materials.

3.4. X-ray diffraction (XRD)

X-ray analysis of extruded starch samples and original starch samples were conducted respectively. X-ray diffraction patterns of original starch samples were shown in Fig. 5, and patterns of

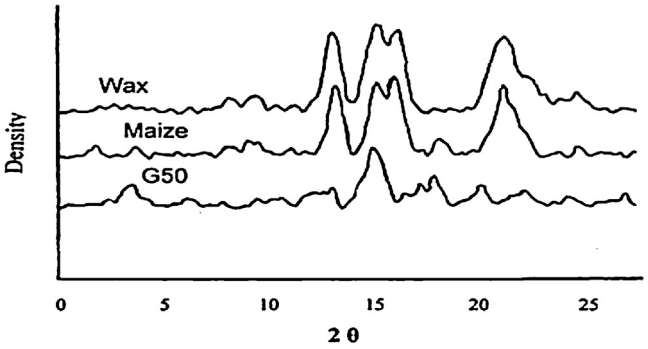

Fig. 5. X-ray diffraction patterns of original starch samples (WAXY, MAIZE, G50).

Table 4
Relative content of different crystals in starch samples.

Crystal type	Corn (%)	G50 (%)	CS (%)	WAXY (%)
B-type	6.76	2.65	0	0
V-type	1.32	1.51	2.12	0
Microcrystal	8.08	4.16	2.12	0
Crystallinity index	65.76	63.60	63.64	63.11

extruded starch samples were shown Fig. 6. According to X-ray diffraction patterns, relative contents of crystals in extruded starch samples were shown in Table 4.

3.5. Correlations between SPAM images and crystal structure of extruded starch samples

When scanning extruded starch samples to acquire SPAM acoustic images, we can obtain mV, which is the image contrast. According to imaging mechanism, mV reveals the difference of elastic properties of measured samples. Yin (Yu & Yin, 2005) studied the SPAM acoustic images of ferroelectric domain, functional ceramics, single crystal and biological tissue. It showed that changes of contrast reflected the microstructure information of material surface and sub-surface (Yin, Yu, Zeng, Li, & Xu, 2005; Yu & Yin, 2005; Zeng, Li, Yin, & Tang, 2003; Zhao, Zeng, & Song, 2009). Sonic wave passed through the boundary between transducer and sample and then spread through the sample. When sonic wave encountered the heterogeneity of material microstructure and properties such as inhomogeneous composition, micro defect, domain structure, crystal grain, grain boundary and grain orientation, it would reflect, refract, or its strength would be changed, thus alternating the way microcantilever vibrated.

Table 5
Samples with different amylose content and sample contrast.

Parameters	WAXY	CS, corn	G50
Amylose content	0	0.26	0.50
Contrast	80.5	133.7	235.0

To figure out correlations between starch structure and SPAM images, 132,000 signals collected from each acoustic image of extruded starch samples were “40 values” processed, and the relationship of contrast and contrast distribution density were obtained, which shown in Fig. 7. These curves matched the X-ray diffraction patterns in Fig. 6A–C very well, which indicated the distinct relevance between acoustic image contrast and crystal structure, crystal content and elastoplasticity of starch material. Apart from being influenced by the uneven height of material surface, contrast was also changed by the different elastoplasticity of measured zones which resulted from the heterogeneous starch crystal components. As a result, acoustic images revealed the difference of distribution density of starch crystals.

3.6. Correlation between acoustic image contrast and amylose content

Average the contrast of acoustic image of the same samples, as shown in Table 5 and then amylose content of samples and image contrast were analyzed linearly, acquired curve was shown in Fig. 6.

As revealed in Table 5 and Fig. 8, for extruded starch samples, there was a good linear relationship between acoustic image contrast and amylose content.

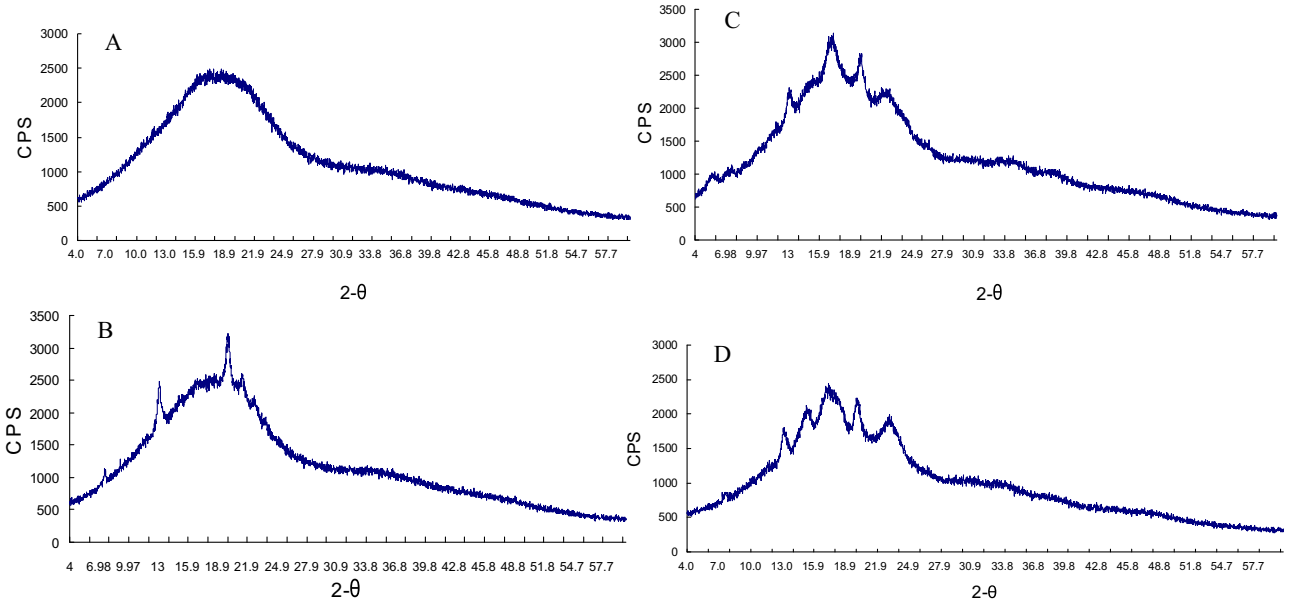

Fig. 6. X-ray diffraction patterns of extruded starch sample WAXY (A), sample CS (B), sample G50 (C) and sample corn (D).

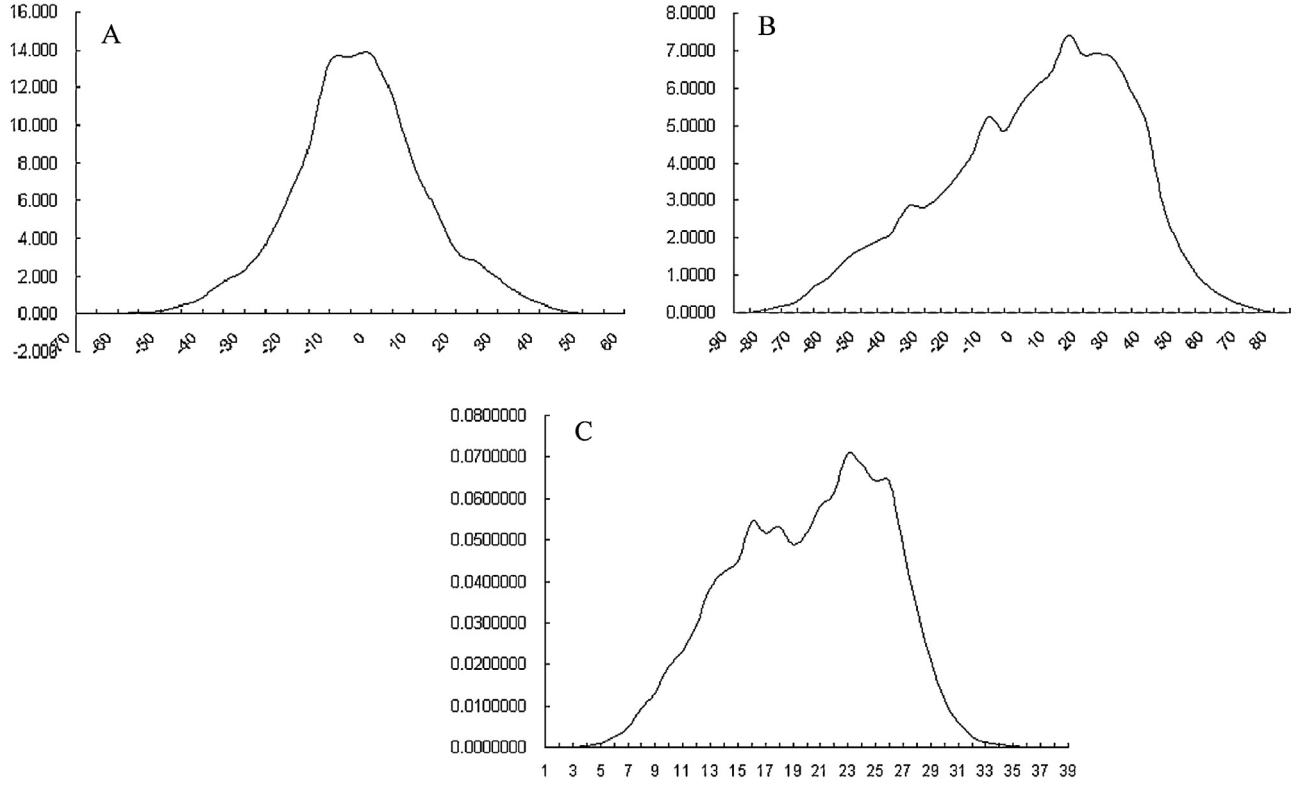

Fig. 7. Contrast–contrast density relationship of sample WAXY (A), sample CS (B) and sample G50 (C).

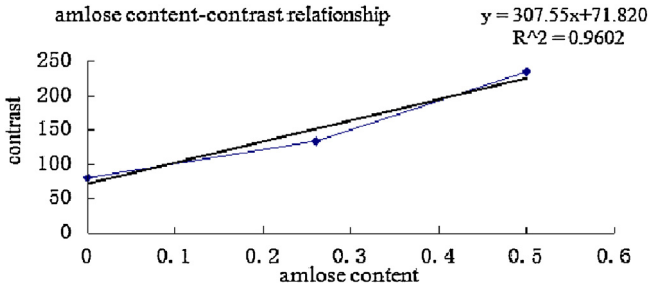

Fig. 8. Relationship between contrast and amylose content.

4. Conclusions

This work established the SPAM imaging method to characterize visual crystal structure of starch materials, discovered the correlations between crystal state and acoustic image of starch materials and broadened the application of acoustic microscopy. Sample preparation method is suitable for extruded starch material of soft matter properties. After polishing, clear acoustic images could be obtained under the following circumstances:

1) Vickers hardness value is above 166;
2) the accumulative bright region areas does not exceed 5.7 μm^2 in any $r = 1.5$ mm circle;
3) the accumulative particle projection region area does not exceed 0.3 μm^2 in any $r = 1.5$ mm circle.

SPAM acoustic images of extruded starch material provided visual evidence of starch crystal, reflected the starch crystallinity index, aggregation of crystals, discrete degree and relative content of microcrystal and helped us "see" starch clearly in mesoscopic scale.

SPAM acoustic image contrast had a linear relationship with amylose content of starch materials.

Acknowledgements

This work is supported by National Natural Science Foundation of China (NSFC) (Nos. 11079019, 3107606, 11111120315, 31071606, 11111120315 and 31211120015), Shanghai Synchrotron Radiation Facility (SSRF) and the National Synchrotron Radiation Laboratory (NSRL).

References

An, H. J., Liang, H. L., & Liu, Z. D. (2011). Nano-structures of debranched potato starch obtained by isoamylolysis. *Journal of Food Science*, *76*, 11–14.

Baldwin, P. M., Adler, J., Davies, M. C., & Melia, C. D. (1998). High resolution imaging of starch granule surfaces by AFM. *Journal of Cereal Science*, *27*, 255–265.

Gallant, D. J., Bouchet, B., & Baldwin, P. M. (1997). Microscopy of starch: Evidence of a new level of granule organization. *Carbohydrate Polymers*, *32*, 177–191.

Guo, Y. C., Liu, Z. D., An, H. J., Li, M. Q., & Hu, J. (2011). Nano-structure and properties of maize zein studied by atomic force microscopy. *Journal of Cereal Science*, *76*, 11–14.

Hug-Iten, S., Handschin, S., Conde-Petit, B., & Escher, F. (1999). Changes in starch microstructure on baking and staling of wheat bread. *LWT – Food Science and Technology*, *32*, 255–260.

Deborah Le Corre, Bras, J., & Dufresne, A. (2010). Starch nanoparticles: A review. *Biomacromolecules*, *11*, 1139–1153.

Li, H., Liu, Z. D., & Liu, B. X. (2009). Application of the molecular combing technique to starch granules. *Molecules*, *14*, 4079–4086.

Ridout, M. J., Gunning, A. P., Parker, M. L., Wilson, M. L., & Morris, V. J. (2002). Using AFM to image the internal structure of starch granules. *Carbohydrate Polymers*, *50*, 123–132.

Thiré, R. M. S. M., Simão, R. A. S., & Andrade, C. T. (2003). High resolution imaging of the microstructure of maize starch films. *Carbohydrate Polymers*, *54*, 149–158.

Yin, Q. R., Yu, H. F., Zeng, H. R., Li, G. R., & Xu, Z. K. (2005). SFM in acoustic mode and its applications to observation of ferroelectric domain. *Materials Science and Engineering B*, *120*, 100–103.

Yu, H. F., & Yin, Q. R. (2005). Scanning probe acoustic microscopy of ferroelectrics. *Journal of Sichuan University*, *42*, 99–101.
Zeng, H. R., Li, G. R., Yin, Q. R., & Tang, X. G. (2003). SFM investigation of nanoscale domain structure in ferroelectric PZT thin films. *Acta Physica Sinica*, *52*, 1783–1787.
Zhao, K. Y., Zeng, H. R., & Song, H. (2009). Nanoscale elastic response of grain boundaries in ZnO varistors by acoustic mode AFM. *Journal of Inorganic Materials*, *24*, 869–872.
Zobel, H. F. (1988). Starch gelatinization: An X-ray diffraction study. *Starch/Starke*, *40*, 1–7.